DALTON
FULL PAPER

Structural study of the trigonal $Bi_{2.34}U_{0.33}La_{0.33}O_5$ oxide ion conductor: Rietveld refinement of X-ray and neutron powder diffraction data

Jose Manuel Amarilla, Jose Antonio Alonso and Rosa M. Rojas*

Instituto de Ciencia de Materiales de Madrid, C.S.I.C., Cantoblanco, 28049 Madrid, Spain

Received 11th August 1998, Accepted 1st February 1999

The structure of $Bi_{2.34}U_{0.33}La_{0.33}O_5$ has been investigated by Rietveld refinement of powder X-ray and neutron diffraction data. The compound is trigonal, space group $P\bar{3}$, $Z = 1$, and lattice parameters $a_H = 4.01395(8)$, $c_H = 9.5423(2)$ Å. X-Ray diffraction data are in favour of a model in which U and La atoms are situated in different crystallographic positions: *i.e.* 1a and 2d of the $P\bar{3}$ space group respectively, forming mixed Bi/U and Bi/La layers which alternate along the *c* axis. The structure of this bismuth-based mixed oxide can be described as built up of interlocked edge-sharing $(Bi/U)O_8$ and $(Bi/La)O_8$ polyhedra. The co-ordination polyhedron around the Bi/U atoms is a hexagonal bipyramid, the equatorial plane being a puckered hexagon. The Bi/La atoms are co-ordinated to eight oxygen atoms forming a slightly distorted cube. Electron diffraction studies showed that the structure can be described as a fluorite-type superstructure, the relation to the fluorite sub-cell is $\boldsymbol{a}^*_H \approx \frac{1}{3}[\bar{2}\,\bar{2}4]\boldsymbol{a}^*_C$, $\boldsymbol{b}^*_H \approx \frac{1}{3}[\bar{4}22]\boldsymbol{a}^*_C$, $\boldsymbol{c}^*_H \approx \frac{1}{3}[111]\boldsymbol{a}^*_C$. This compound is a good oxide ion conductor ($\sigma_{300\,°C} = 2.5 \times 10^{-5}$ S cm^{-1}). On the basis of the anion vacancies distribution determined from neutron diffraction refinement, a pathway for the oxide ion conduction is proposed.

The high-temperature cubic fluorite-type modification of bismuth sesquioxide (δ-Bi_2O_3) is the best solid-state oxide-ion conductor, the conductivity being about two orders of magnitude higher than that of conventional oxide conductors such as stabilized zirconia.[1] The structure of this oxide, in which the anion network contains 25% intrinsic vacancies, accounts for the high conductivity of δ-Bi_2O_3. The cubic phase is only stable between 728 °C and the melting point at 824 °C. However, stabilization at room temperature of δ-Bi_2O_3 can be attained by addition of several oxides.[2] Owing to the high oxide-ion conductivity, materials based on cubic Bi_2O_3 are very promising as solid electrolytes in electrochemical devices such as low-temperature solid oxide fuel cells (LT-SOFCs)[3] and oxygen pumps.[4] It has been shown that many of the stabilized δ phases are quenched high-temperature phases, and by annealing they are transformed into the low-temperature stable phases. However, in some cases, doping with aliovalent cations allows the oxide to retain the cubic δ phase after annealing even for more than 1500 h.[5,6]

In previous papers[7,8] we have reported on the synthesis of new bismuth-based oxide materials of general formula $Bi_{2-2x}U_xLa_xO_{3+3x/2}$ ($0.038 \leq x \leq 0.333$). For the material with $x = 0.222$ ($Bi_{1.56}U_{0.22}La_{0.22}O_{3.33}$) three different polymorphs have been identified. The trigonal polymorph, which is the room temperature stable phase, has lattice constants $a_H = 4.01395(8)$, $c_H = 9.5423(2)$ Å. The X-ray pattern of this polymorph closely resembles that of the high-temperature modification of Bi_2UO_6,[9] space group $P\bar{3}$. The cubic polymorph, which is obtained by quenching of the trigonal phase from 950 °C, has the fluorite-type structure with lattice parameter $a_C = 5.6273(8)$ Å. The monoclinic polymorph with lattice parameters $a_M = 7.778(3)$, $b_M = 7.834(4)$, $c_M = 5.763(3)$ Å, $\beta = 89.71(2)°$ is obtained on annealing both the trigonal and cubic polymorphs at 600 °C for 500 h. This monoclinic phase is the one obtained by annealing all other compositions studied in the $Bi_{2-2x}U_xLa_xO_{3+3x/2}$ ($0.038 \leq x \leq 0.333$) system, either mixed with the corresponding hexagonal phase and/or α-Bi_2O_3.[8]

The oxide-ion conductivity shown by the several $Bi_{1.56}U_{0.22}La_{0.22}O_{3.33}$ polymorphs is rather different.[7] At 300 °C the monoclinic phase shows the lowest conductivity, $\sigma = 6.6 \times 10^{-7}$ S cm^{-1}. For the trigonal polymorph a remarkable increase of conductivity by two orders of magnitude is observed, $\sigma = 2.5 \times 10^{-5}$ S cm^{-1}. The conductivity for the cubic phase, which is the best, is 7.2×10^{-5} S cm^{-1}. The conductivity properties of these materials is due to the O^{2-} ions mobility through the oxygen vacancies, 16.5% in this oxide. Therefore the understanding of the conduction mechanism requires an accurate knowledge of the oxygen positions and their population, *i.e.* the O^{2-} vacancy distribution. We have undertaken the crystal structure determination of the room-temperature stable $Bi_{1.56}U_{0.22}La_{0.22}O_{3.33}$ polymorph by Rietveld refinement of powder neutron and X-ray diffraction data. On the basis of oxygen vacancy distribution, a mechanism in which the oxide ions situated between the mixed Bi/U and Bi/La layers would be the most involved in the conduction process is proposed.

Results

Structural analysis and refinement

The structure of trigonal $Bi_{1.56}U_{0.22}La_{0.22}O_{3.33}$ was analysed by profile refinement of both neutron and X-ray diffraction data. Having in mind the similarities between the X-ray pattern of this polymorph and that of the high-temperature modification of Bi_2UO_6,[9] the structure analysis of the $Bi_{1.56}U_{0.22}La_{0.22}O_{3.33}$, that may be better formulated as $Bi_{2.34}U_{0.33}La_{0.33}O_5$, was made assuming the $P\bar{3}$ space group, and the initial atomic positions were deduced from the trigonal Bi_2UO_6.

For the neutron refinement, considering the close values of the coherent neutron scattering lengths of the cations involved ($b_U = 8.42$, $b_{Bi} = 8.5$, $b_{La} = 8.24$ fm), bismuth, uranium and lanthanum were randomly distributed between the 2d and 1a positions of the $P\bar{3}$ group, with population factors of 2 and 1, respectively. The five oxygen atoms were averaged distributed between the 2d and 2c sites, with occupancy 1.66. The final Rietveld refinement involved the appropriate atomic parameters and displacement factors, the oxygen occupancy, the lattice constants, the zero point, the scale factor, the profile parameters, and the background parameters.

Table 1 Structural parameters and *R* factors for $Bi_{2.34}U_{0.33}La_{0.33}O_5$ from Rietveld refinement of the neutron diffraction data

Atom	Wyckoff symbol	*x*/*a*	*y*/*b*	*z*/*c*	*B*/Å²	Occupancy
M(1)[a]	2d	2/3	1/3	0.3464(2)	1.64(3)	2
M(2)[a]	1a	0	0	0	2.78(7)	1
O(1)	2d	2/3	1/3	0.025(1)	11.4(4)	1.61(8)
O(2)	2d	2/3	1/3	0.580(4)	7.3(2)	1.92(1)
O(3)	2c	0	0	0.2290(6)	4.9(2)	1.51(5)

[a] In accord with Rietveld refinement of X-ray diffraction data, M(1) and M(2) stand for (Bi/La) and (Bi/U) atoms, respectively, in the stoichiometric relationships. No. refined parameters: 20. Space group $P\bar{3}$ (no. 147), $Z = 1$, $a_H = 4.01395(8)$, $c_H = 9.5423(2)$ Å, $\lambda = 1.594$ Å, $R_B = 7.15$, $R_p = 3.45$, $R_{wp} = 4.44$, $R_{exp} = 3.02\%$, $\chi^2 = 2.16$.

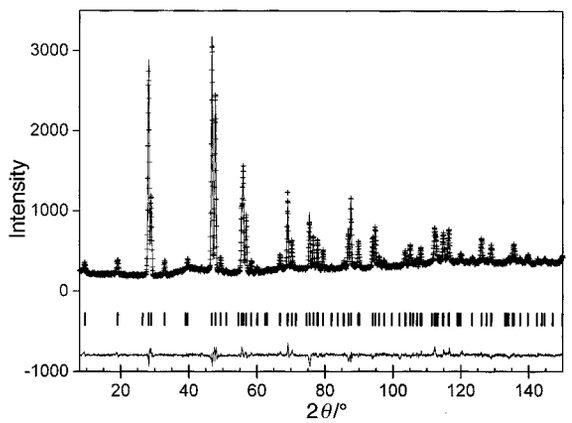

Fig. 1 Rietveld fit for trigonal $Bi_{2.34}U_{0.33}La_{0.33}O_5$, neutron data. Crosses represent the observed data, the solid line is the calculated pattern, and the difference profile and allowed reflections are shown beneath.

The observed, calculated and difference profiles for the neutron diffraction pattern are shown in Fig. 1. The results of the neutron Rietveld refinement are presented in Table 1. A good agreement between the calculated and experimental profiles is obtained as shown by the low *R* factors. The latest refinement has shown a correlation between the oxygen displacement factor and the occupancy, that makes difficult the accurate determination of the oxygen occupancy. However, the values obtained for this parameter (Table 1) clearly show that the oxide ions are not equally distributed at the 2d and 2c sites, the occupancy being always significantly higher for the O(2) at the 2d position (2/3, 1/3, $z = 0.5798$) than for O(1) and O(3) at (2/3,1/3, $z = 0.025$) and (0,0, $z = 0.229$), respectively. The displacement factors for the oxygen atoms are large, particularly that of the O(1), $B = 11.4$ Å². It is worth mentioning that large *B* values have also been determined for oxygen atoms in several bismuth-based oxide ion conductors. The high displacement factors found for this compound are not unusual in highly defective materials such as doped Bi_2O_3. Reported values range from 13.7(7) for δ-Bi_2O_3 [10] to 7.5(2) Å² for $(Bi_2O_3)_{0.80}(Er_2O_3)_{0.20}$ [11] and 5.67(87) Å² for $Bi_{0.7}La_{0.3}O_{1.5}$.[12]

The neutron diffraction experiment cannot discriminate among bismuth, lanthanum and uranium. X-Ray diffraction can act as a complementary technique since the atomic numbers of lanthanum, bismuth and uranium are in such a relation that it could be possible to distinguish among them. For the Rietveld refinement of the X-ray diffraction profile the atomic positions, the displacement factors *B*, and the oxygen occupancy determined from neutron refinement were not refined. Several bismuth, uranium and lanthanum distributions between the 2d and 1a positions were considered, and the fitting of the profile was undertaken on the basis of the following models consistent with the stoichiometry of the material: (A) $[Bi_{1.56}U_{0.22}La_{0.22}]_{2d}[Bi_{0.78}U_{0.11}La_{0.11}]_{1a}$, fully random cation distribution; (B) $[Bi_2]_{2d}[Bi_{0.34}U_{0.33}La_{0.33}]_{1a}$, uranium and lanthanum situated at the 1a site; (C) $[Bi_{1.34}U_{0.33}La_{0.33}]_{2d}[Bi_1]_{1a}$, uranium and lanthanum situated at the 2d site; (D) $[Bi_{1.67}La_{0.33}]_{2d}$-$[Bi_{0.67}U_{0.33}]_{1a}$, lanthanum situated at the 2d site and uranium at the 1a site; (E) $[Bi_{1.67}U_{0.33}]_{2d}[Bi_{0.67}La_{0.33}]_{1a}$, the uranium and lanthanum atoms are positioned at the 2d and 1a sites, respectively. The reliability factors obtained for each cation distribution are outlined in Table 2. In any case, the values of the *R* factors are low, even though a variation depending on the model considered is observed. In Fig. 2 the experimental, calculated and difference profiles obtained for model D, which is the one that best fit the experimental data, are presented.

Table 2 Reliability factors obtained from the Rietveld X-ray powder profile refinement for the different cation distribution models

Cation distribution	$R_{Bra.}$(%)	R_p (%)	R_{wp} (%)	χ^2
(A) $[Bi_{1.56}U_{0.22}La_{0.22}]_{2d}[Bi_{0.78}$-$U_{0.11}La_{0.11}]_{1a}$	9.41	7.01	9.41	9.53
(B) $[Bi_2]_{2d}[Bi_{0.34}U_{0.33}La_{0.33}]_{1a}$	9.88	7.19	10.2	11.3
(C) $[Bi_{1.34}U_{0.33}La_{0.33}]_{2d}[Bi_1]_{1a}$	9.16	6.96	9.23	9.17
(D) $[Bi_{1.67}La_{0.33}]_{2d}[Bi_{0.67}U_{0.33}]_{1a}$	9.14	6.90	9.10	8.91
(E) $[Bi_{1.67}U_{0.33}]_{2d}[Bi_{0.67}La_{0.33}]_{1a}$	10.1	7.61	11.9	15.4

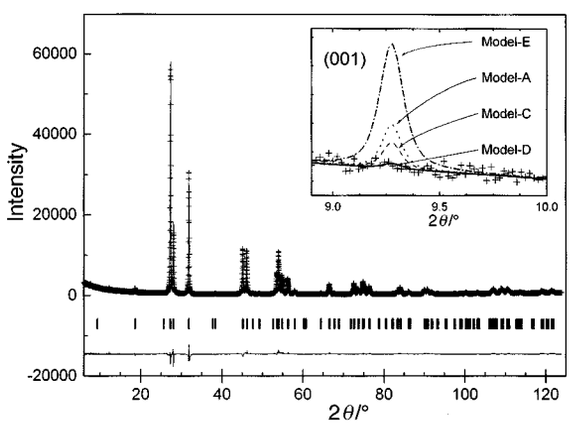

Fig. 2 Rietveld fit for trigonal $Bi_{2.34}U_{0.33}La_{0.33}O_5$, X-ray data. The inset shows the enlarged 9–10° 2θ region, and the fit of the (001) reflection by the indicated cation distribution model.

An electron diffraction study has also been carried out on this material. In Fig. 3 selected area electron diffraction patterns taken on the trigonal $Bi_{2.34}U_{0.33}La_{0.33}O_5$ are shown. The strong Bragg spots can be indexed on the basis of a fluorite-type sub-cell, space group $Fm\bar{3}m$, $a_C = 5.63$Å, along the $[\bar{1}\,\bar{1}\,2]_C$ and $[\bar{1}10]_C$ zone axes. However, the values of some interplanar angles evidence the distortion of the cubic symmetry. In addition, several superlattice spots at 1/3 and 2/3 along $\langle 111\rangle^*_C$ and $\langle \bar{2}\,\bar{2}4\rangle^*_C$ of the fluorite basic cell are observed. The patterns can be better indexed on the basis of the hexagonal cell deduced from X-ray and neutron diffraction patterns. Relationships between the fluorite and the hexagonal unit cells are as follows: $\boldsymbol{a}^*_H = \frac{1}{3}[\bar{2}\,\bar{2}4]\boldsymbol{a}^*_C$, $\boldsymbol{b}^*_H = \frac{1}{3}[\bar{4}22]\boldsymbol{b}^*_C$ and $\boldsymbol{c}^*_H = \frac{1}{3}[111]\boldsymbol{c}^*_C$. The unit cell vectors in reciprocal space can be taken as: $\boldsymbol{a}^*_H = -\frac{2}{3}\boldsymbol{a}^*_C - \frac{2}{3}\boldsymbol{b}^*_C + \frac{4}{3}\boldsymbol{c}^*_C$, $\boldsymbol{b}^*_H = -\frac{4}{3}\boldsymbol{a}^*_C + \frac{2}{3}\boldsymbol{b}^*_C + \frac{2}{3}\boldsymbol{c}^*_C$ and $\boldsymbol{c}^*_H = \frac{1}{3}\boldsymbol{a}^*_C + \frac{1}{3}\boldsymbol{b}^*_C + \frac{1}{3}\boldsymbol{c}^*_C$ where $\boldsymbol{a}^*_C$, $\boldsymbol{b}^*_C$ and $\boldsymbol{c}^*_C$ are the reciprocal unit cell vectors of the fluorite-type basic cell. The deduced real unit cell vectors are: $\boldsymbol{a}_H = -\frac{1}{2}\boldsymbol{b}_C + \frac{1}{2}\boldsymbol{c}_C$, $\boldsymbol{b}_H = -\frac{1}{2}\boldsymbol{a}_C + \frac{1}{2}\boldsymbol{b}_C$ and $\boldsymbol{c}_H = \boldsymbol{a}_C +$

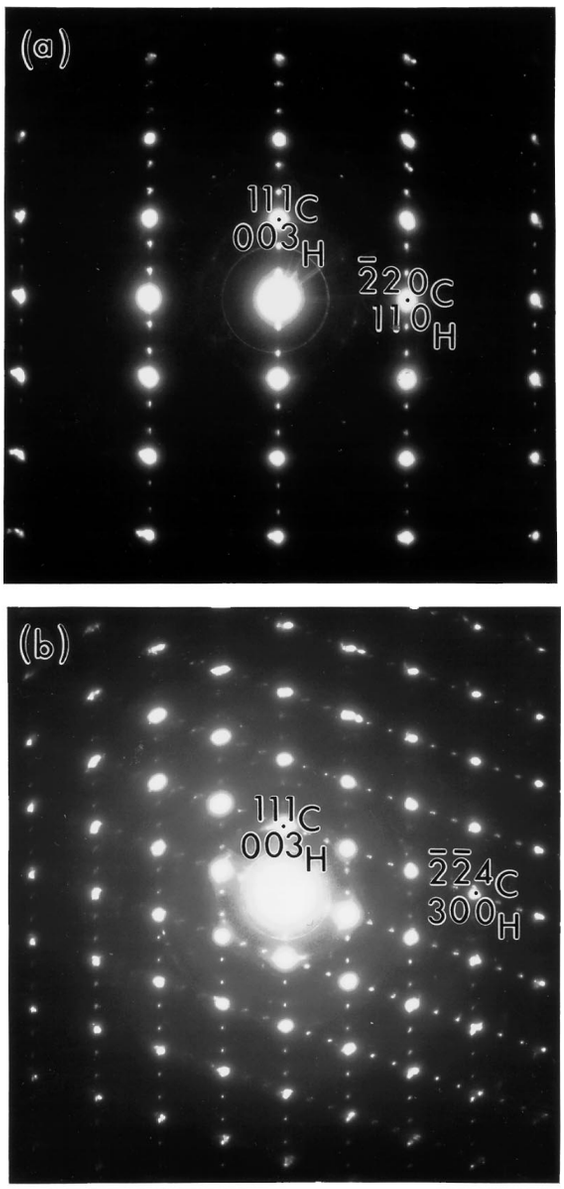

Fig. 3 Selected area electron diffraction patterns for $Bi_{2.34}U_{0.33}La_{0.33}O_5$ along the zone axes: (a) $[\bar{1}\,\bar{1}\,2]_C \parallel [\bar{1}\,1\,0]_H$; (b) $[\bar{1}\,1\,0]_C \parallel [0\,1\,0]_H$; C and H stand for cubic and hexagonal, respectively.

$\boldsymbol{b}_C + \boldsymbol{c}_C$. From these expressions, the lattice parameters of the trigonal $Bi_{2.34}U_{0.33}La_{0.33}O_5$ can be related with the cubic fluorite-type structure as follows: $a_H = a_C\sqrt{2}/2$; $b_H = a_C\sqrt{2}/2$; $c_H = a_C\sqrt{3}$. The calculated lattice parameters $a_H = b_H \approx 3.98$, $c_H \approx 9.75$ Å are in good agreement with those determined from the powder X-ray diffraction pattern.

Discussion

The structural model considered for trigonal $Bi_{2.34}U_{0.33}La_{0.33}O_5$, derived from the high-temperature modification of Bi_2UO_6, fits well both X-ray and neutron diffraction data as shown by the low values of the reliability factors *R* (Tables 1 and 2). The Rietveld refinement of the X-ray diffraction profile show that the *R* factors vary with the cation distribution (Table 2), indicating that X-ray diffraction is sensitive to the distribution of the heavy atoms in this compound. It is worth noting that when lanthanum, which is the metal atom with less electrons, is placed at the 1a site, models A, B and E, the reliability factors show a worse fit of the X-ray diffraction data. A detailed study of the profiles calculated for the five models has revealed that some reflections are particularly sensitive to the cation distribution, *i.e.* the (001) at 2θ 9.25°, as shown in the inset in Fig. 2. In this inset the X-ray diffraction profiles calculated for models (A) $[Bi_{1.56}U_{0.22}La_{0.22}]_{2d}[Bi_{0.78}U_{0.11}La_{0.11}]_{1a}$, (C) $[Bi_{1.34}La_{0.33}U_{0.33}]_{2d}$-$[Bi_1]_{1a}$, (D) $[Bi_{1.64}La_{0.33}]_{2d}[Bi_{0.67}U_{0.33}]_{1a}$ and (E) $[Bi_{1.67}U_{0.33}]_{2d}$-$[Bi_{0.67}La_{0.33}]_{1a}$ are compared to the experimental data. For model E, in which all lanthanum is placed at the 1a site, the (001) reflection shows a noticeable intensity. In the profile calculated from model D the (001) reflection is practically non-observed as it is in the experimental pattern (see inset in Fig. 2). This model is the one that best fits the experimental X-ray profile.

Table 3 Bond lengths (Å) and angles (°) for trigonal $Bi_{2.34}U_{0.33}$-$La_{0.33}O_5$[a]

$[M(1)O_8]$ polyhedra		$[M(2)O_8]$ polyhedra	
M(1)–O(1) × 6	2.329(1)	M(2)–O(1) × 1	3.07(1)
M(1)–O(3) × 2	2.185(5)	M(2)–O(2) × 1	2.228(4)
⟨M(1)–O⟩	2.293(2)	M(2)–O(2) × 3	2.422(1)
		M(2)–O(3) × 3	2.574(2)
		⟨M(2)–O⟩	2.536(3)
O(1)···O(3)	3.028(7)	O(1)···O(3)	3.028(7)
O(1)···O(1)	2.365(3)	O(2)···O(2)	2.773(3)
O(1)···O(3)	3.351(8)	O(2)···O(3)	2.950(4)
O(1)–O(3)–O(1)	82.81	O(3)–O(1)–O(3)	83.02
O(3)–O(1)–O(1)	75.82	O(1)–O(3)–O(2)	95.60
O(1)–O(1)–O(1)	116.08	O(3)–O(2)–O(3)	85.75
		O(2)–O(2)–O(2)	92.72
		O(2)–O(2)–O(3)	90.64
		O(2)–O(3)–O(2)	85.75

[a] M(1) and M(2) stand for (Bi/U) and (Bi/La) mixed layers at 1a and 2d sites, respectively.

In Table 3 the metal–oxygen and oxygen–oxygen bond lengths and angles are presented. In Fig. 4 a representation of the arrangement of the co-ordination polyhedra in the trigonal $Bi_{2.34}U_{0.33}La_{0.33}O_5$ unit cell is depicted. The structure can be described as built up of interlocked edge-sharing $[M(1)O_8]$ and $[M(2)O_8]$ polyhedra. In this structure one M(1) layer alternates along the *c* axis with two M(2) layers. In the former, cations are surrounded by a highly distorted oxygen cube flattened along the 3-fold axis, the metal atoms being bonded to two oxide ions O(3) at 2.185(5) Å and to six O(1) at 2.329(1) Å. This $[M(1)O_8]$ polyhedron can be better described as a hexagonal bipyramid, the equatorial plane being a puckered hexagon chair formed by six O(1) atoms, perpendicular to the O(3)–M–O(3) axis [Fig. 4(b)]. The U^{6+} is a relatively small (0.86 Å)[13] highly charged cation, therefore the presence of uranium in the M(1) layer would account for the high distortion of the cube, as well as for the shortest M(1)–O distance in the structure, M(1)–O(3) 2.185(5) Å. A similar co-ordination polyhedron has been found in many U^{6+} compounds such as alkaline-earth metal uranates, uranyl carboxylates, uranyl nitrates, *etc.*[14,15] It can be pointed out that model D, in which uranium atoms adopt this hexagonal bipyramidal co-ordination, and is the one that better fits the experimental X-ray data, gives the most plausible distribution of cations in the structure. It follows that we are dealing with a cation distribution in which uranium and lanthanum are situated in different crystallographic positions, *i.e.* 1a and 2d, respectively. Bismuth ions are distributed between both positions to attain the total occupancy of each crystallographic site.

In the mixed M(2) layer the atoms are bonded to eight oxygen atoms situated at the corners of a slightly distorted cube [Fig. 4(c)]. Note that average ⟨M(2)–O⟩ bond lengths are significantly larger than ⟨M(1)–O⟩ distances (Table 3). It is reasonable to assume that La^{3+} with larger ionic radius (1.10 Å) with respect to U^{6+} (0.86 Å) is placed in the M(2) mixed layer. The O···O bond distances in the $[(Bi/La)O_8]$ polyhedron range from 2.77 to 3.03 Å, and bond angles are about 90°. It is worth noting that the metal atoms are significantly shifted away from the geometrical centre of the cube, giving a short (Bi/La)–O(2)

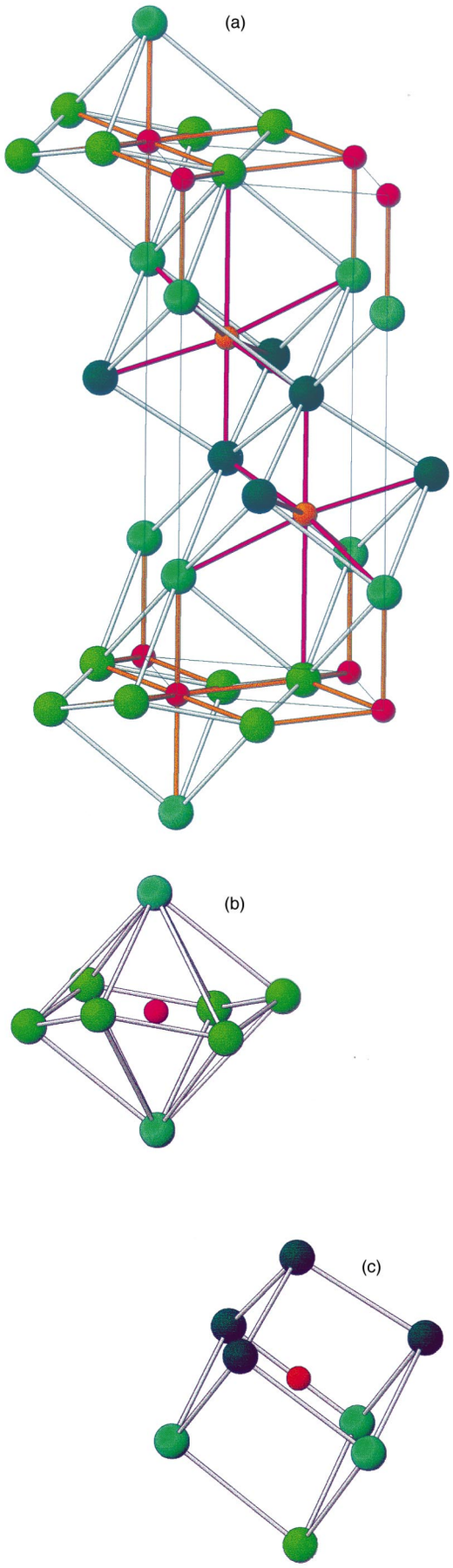

Fig. 4 Crystal structure of trigonal $Bi_{2.34}U_{0.33}La_{0.33}O_5$ showing: (a) the arrangement of the co-ordination polyhedra of the cations in the unit cell; (b) $(Bi/U)O_8$ polyhedron; (c) $(Bi/La)O_8$ polyhedron. Key: red, Bi/U; orange, Bi/La; light green, O(1); dark green, O(2); medium green, O(3).

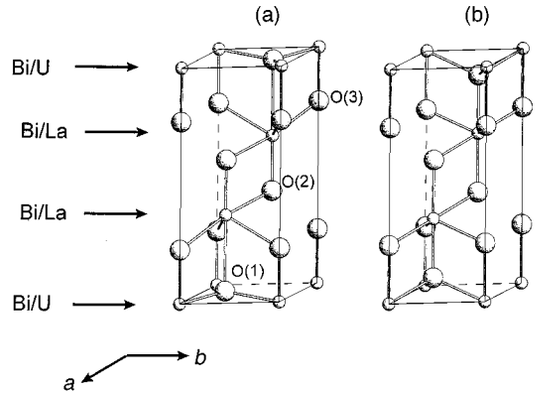

Fig. 5 (a) $Bi_{2.34}U_{0.33}La_{0.33}O_5$ unit cell. (b) Hexagonal cell derived for the fluorite-type cell. In (a) the atoms are as indicated, in (b) the bigger balls stand for anions and the small ones represent the metal ions.

and long (Bi/La)–O(1) distances of 2.228(4) and 3.07(1) Å, respectively. The presence of several Bi–O distances is not unusual for trivalent bismuth compounds, and our values are within those determined for several bismuth oxides.[9,10,16,17] The irregular co-ordination observed in many Bi^{3+}-containing compounds is attributed to the stereochemical effect of the lone electron pair on Bi^{3+}.[18,19]

Electron diffraction studies show that the structure of this trigonal polymorph can be related with the fluorite-type structure. In fact, this compound reversibly transforms on heating above 950 °C to a faced-centred cubic (f.c.c.) phase.[8] A simple operation transforms a f.c.c.-type cell into a hexagonal cell: $a_H = b_H = a_C\sqrt{2}/2$, $c_H = a_C\sqrt{3}$; $V_H = \frac{3}{4}V_C$. The a_H and c_H parameters of the hexagonal cell derived for the fluorite-type structure have been calculated from the lattice constant of the cubic $Bi_{2.34}U_{0.33}La_{0.33}O_5$ polymorph obtained at $T > 950$ °C, $a_C = 5.6273(8)$ Å. In Fig. 5 the unit cell of the trigonal $Bi_{2.34}U_{0.33}La_{0.33}O_5$ polymorph is compared with the hexagonal cell derived for the fluorite-type structure. From these drawings it follows that the trigonal and cubic structures are closely similar. However, some differences have to be noticed: (i) the metal atoms at (2/3,1/3, $z = 1/3$) in the fluorite cell [Fig. 5(b)] are now at $z = 0.3464(4)$. This means that in trigonal $Bi_{2.34}U_{0.33}La_{0.33}O_5$ the mixed (Bi/La) layers are closer to each other than in the fluorite structure, and further away from the (Bi/U) layer. (ii) The O(1) atoms are shifted away from their positions in the fluorite lattice. They come closer to the (Bi/U) layer as shown by the value of the angle (Bi/U)–O(1)–(Bi/La) 95.84°, significantly lower than the 109.45° for tetrahedral co-ordination of oxygen in the fluorite-type cell. (iii) The O(3) atoms are only slightly shifted, getting closer to the mixed (Bi/U) layer at (0,0,0), and giving the shortest M–O distance in the structure. As a result, the shifting of the atoms from their equilibrium positions in the fluorite-type cell causes distortion of both the tetrahedral and cubic co-ordination polyhedra of the oxide and metal atoms, giving the formation of the trigonal $Bi_{2.34}U_{0.33}La_{0.33}O_5$ polymorph that can be described as a fluorite superstructure.

We have previously studied the electrical properties of trigonal $Bi_{2.34}U_{0.33}La_{0.33}O_5$.[7] The conductivity at 300 °C ($\sigma_{300\,°C} = 2.5\ 10^{-5}$ S cm^{-1}) shows that this material is a good solid ionic conductor. The conductivity is assigned to the O^{2-} motion through the anion vacancies in the oxygen network. The Rietveld refinement of the neutron diffraction data shows that the oxide ions are not equally distributed at the 2d and 2c sites, the occupancy being always significantly higher for the O(2) than for O(1) and O(3). Provided that the anion vacancies are preferentially located at the (Bi/U)–O network, and taking into account the large displacement factor of O(1) oxygens, $B = 11.4(4)$ Å^2, it is plausible to assume that the pathway of conduction goes through the O(1)–O(3) sites. This mechanism

implies that trigonal $Bi_{2.34}U_{0.33}La_{0.33}O_5$ can be considered as a two-dimensional ionic conductor.

Experimental

The trigonal $Bi_{2.34}U_{0.33}La_{0.33}O_5$ polymorph was synthesized by heating at 950 °C for 24 h a stoichiometric mixture of monoclinic α-Bi_2O_3 (Fluka) and lanthanum uranate, $LaUO_{4+x}$. The latter compound was previously obtained by thermal decomposition at 850 °C of lanthanum uranyl propionate, $LaUO_2(C_2H_5CO_2)_5 \cdot 3H_2O$. The reaction mixture was kept at 950 °C for 24 h, then slowly cooled at 2 °C h^{-1} to 650 °C and at 1 °C min^{-1} to room temperature. A detailed description of the synthesis procedure has been given elsewhere.[8]

Powder X-ray diffraction patterns were recorded on a Siemens D-501 diffractometer with monochromatic Cu-Kα radiation. The patterns were scanned by steps of 0.02° (2θ) and 5 per step counting time. The scans were made in the range $4 \leqslant 2\theta \leqslant 140°$. Neutron diffraction measurements were recorded on the high-resolution powder diffractometer D2B, $\lambda = 1.594$ Å, at the Institute Laue-Langevin in Grenoble. The step size for the experiment was 0.05° in 2θ and the explored angular range 5–160° (2θ). Both X-ray and neutron diffraction patterns were scanned at room temperature. The data were analysed using the method described by Rietveld[20] with the program FULLPROF.[21] In both cases, a pseudo-Voight function was chosen to generate the shape of the diffraction peaks.

Electron diffraction and microscopy were carried out on a JEOL 2000 FX electron microscope fitted with a double tilting goniometer stage of ±45°. The specimens were crushed and dispersed in acetone, and then transferred to holey carbon-coated copper grids.

Acknowledgements

Financial support by Comisión Interministeral de Ciencia y Tecnología (Project MAT95/0899) is acknowledged. Dr J. M. Amarilla thanks the Consejo Superior de Investigaciónes Cientificas for a contract under the mentioned project. We thank Mr A. García Delgado for technical assistance with the electron microscope.

References

1 T. Takahashi and H. Iwahara, *Mater. Res. Bull.*, 1978, **13**, 1447.
2 P. Shuk, H.-D. Wiemhöfer, U. Guth, W. Göpel and M. Greenblatt, *Solid State Ionics*, 1996, **89**, 179.
3 A. M. Azad, S. Larose and S. A. Akbar, *J. Mater. Sci.*, 1994, **29**, 4135.
4 E. N. Naumovich, V. V. Kharton, V. V. Samokhval and A. V. Kovalevsky, *Solid State Ionics*, 1997, **93**, 95.
5 K. Z. Fung and A. V. Virkar, *J. Am. Ceram. Soc.*, 1991, **74**, 1970.
6 K. Huang, M. Feng and J. B. Goodenough, *Solid State Ionics*, 1996, **89**, 17.
7 J. M. Amarilla, R. M. Rojas and J. M. Rojo, *Chem. Mater.*, 1998, **10**, 574.
8 J. M. Amarilla and R. M. Rojas, *Chem. Mater.*, 1996, **8**, 401.
9 A. S. Koster, J. P. P. Renaud and G. D. Rieck, *Acta Crystallogr., Sect. B*, 1975, **31**, 127.
10 H. A. Harwig, *Z. Anorg. Allg. Chem.*, 1978, **444**, 151.
11 M. J. Verkerk, G. M. H van de Velde, A. J. Burggraaf and R. B. Helmholdt, *J. Phys. Chem. Solids*, 1982, **43**, 1129.
12 D. Mercurio, M. El Farissi, J. C. Champarnaud-Mesjard, B. Frit, P. Conflant and G. Roult, *J. Solid State Chem.*, 1989, **80**, 133.
13 R. D. Shannon, *Acta Crystallogr., Sect. A*, 1976, **32**, 751.
14 K. W. Bagnall, *Gmelin Handbook of Inorganic Chemistry*, Uranium Suppl. Vol. C13, Verlag Chemie, Weinheim, 1983.
15 *Comprehensive Inorganic Chemistry*, eds. J. C. Bailar, H. J. Emeléus, R. Nyholm and A. F. Trotman-Dickenson, Pergamon, Oxford, 1975, ch. 45.
16 S. K. Blower and C. Greaves, *Acta Crytallogr., Sect. C*, 1988, **44**, 587.
17 J. Pannetier, D. Tranqui and A. W. Sleight, *Mater. Res. Bull.*, 1993, **28**, 985.
18 N. Kumada, N. Kinomura, P. M. Woodward and A. W. Sleight, *J. Solid State Chem.*, 1995, **116**, 281.
19 J. Geb and M. Jansen, *J. Solid State Chem.*, 1996, **122**, 364.
20 H. M. Rietveld, *J. Appl. Crystallogr.*, 1982, **15**, 430.
21 J. Rodriguez-Carvajal, FULLPROF, PC version, Grenoble, France, 1995.

Paper 8/06343E